0038-075C/97/1626-410–420$03.00/0
Soil Science

June 1997
Vol. 162, No. 6
Printed in U.S.A.

NUMERICAL MODEL OF 3-DIMENSIONAL ANISOTROPIC DEFORMATION AND 1-DIMENSIONAL WATER FLOW IN SWELLING SOILS

P. Garnier[1], E. Perrier[1], R. Angulo Jaramillo[2], and P. Baveye[3]

Current models of water flow in deforming soils generally involve a transformation from spatial to material coordinates. Existing forms of this coordinate transformation either assume that soil deformation is one-dimensional, or that it is isotropic. In the present article, we propose a new expression of the transformation gradient tensor, that allows different extents of deformation in the vertical and horizontal directions. The resulting generalized water flow equation is calibrated with experimental data obtained for one-dimensional vertical infiltration in a bentonite sample. The hydraulic characteristics obtained from this calibration are then used to analyze, via simulations, the sensitivity of water flow to anisotropy in soil deformation. The results indicate that the extent of the lateral deformation strongly influences not only the height of the soil surface, as expected, but also the distribution of water and the total volume of water in a swelling/shrinking soil undergoing infiltration or drainage. Consequently, this lateral deformation should be taken into account explicitly in modeling efforts or in the determination of the hydraulic characteristics of soils that deform anisotropically.

MANY soils, not just fine textured ones, experience volume changes when they absorb water or when they dry. These volume changes are often associated with very steep water content gradients and, in some cases, with the development of networks of cracks.

It has long been recognized that the physical behavior of swelling—or deforming—soils differs significantly from that of nonswelling soils, in particular with respect to the transport of water. Fortunately, the work of Raats and Klute (1969), and Smiles and Rosenthal (1968) showed at an early stage in the research of this process that the traditional equation of water flow in nondeforming soils, the Richards (1931) equation, is still formally applicable in deforming soils, provided one introduces a suitable coordinate transformation. With this transformation, the generalized water flow equation is expressed with respect to a coordinate frame that is fixed relative to the soil phase. This generalized equation may be solved by using the same analytical or numerical techniques that are available for the classical Richards (1931) equation. To compare the outcomes of these solutions to actual measurements, typically carried out in a spaced-fixed or spatial coordinate frame, all that is needed is a transformation back from the referential or material coordinates associated with the soil solid phase, to the spatial coordinates.

Over the years, various alternative definitions of this coordinate transformation have evolved and have been tested experimentally (e.g., Smiles and Rosenthal 1968; Raats and Klute 1969; Philip and Smiles 1969; Smiles 1974; Sposito and Giráldez 1976; Douglas et al. 1980; Giráldez et al. 1983; Baveye et al. 1989; Baveye 1992). This research has been based on the assumption that soil deformation occurs predominately in the vertical direction and that lateral deformations are negligible. This perspective may be appropriate in a wide range of field conditions, but there may be cases where lateral deformations cannot be slighted. For example, the

[1]Laboratoire d'Hydrophysique, ORSTOM, 32, Avenue Henri Varagnat, 93143 Bondy Cedex, France.

[2]Laboratoire d'Etude des Transferts en Hydrologie et Environment, LTHE, UMR (CNRS, INPG, UJF), PB 53, 38041 Grenoble Cedex 9, France.

[3]Laboratory of Environmental Geophysics, Bradfield Hall, Cornell University, Ithaca, NY, 14853-1901. Dr. Baveye is corresponding author. E-mail: pcb2@cornell.edu

Received Aug. 21, 1996; accepted Jan. 31, 1997.

cracks that occur in some deforming soils (e.g., vertisols) are manifestations of significant lateral shrinking. On the other hand, in laboratory experiments with small samples of swelling soils, special precautions usually have to be taken to prevent lateral air gaps or curved sample surfaces that result from lateral shrinking or swelling, respectively.

To describe such situations adequately, one needs a coordinate transformation that accounts for lateral deformations. For most practical purposes, it seems reasonable to assume that lateral deformations are isotropic, following Rijniersce (1983) and Bronswijk (1990). The latter authors introduced a geometry factor, r_s that allows the calculation of vertical and horizontal components of volumetric deformation. Even though none seems to have been developed to date, an extended coordinate transformation could be derived on the basis of such a geometry factor. Elaborating such a transformation was the first objective of the research reported in the present article.

A second objective of our research was to analyze in detail, via computer simulation, the extent to which the value of the geometry factor r_s influences solutions of the generalized water flow equation resulting from adoption of the extended coordinate transformation. Part of the effect of r_s is straightforward to predict. Indeed, any lateral deformation will tend to decrease changes in soil height. However, in general, a sensitivity analysis is needed to determine the nature and extent of the effect of r_s on water content profiles, total amount of water in the soil, or value of the hydraulic conductivity at various stages of infiltration or evaporation events.

THEORY

Fundamental Water Flow Equation in Deforming Porous Media

The Richards equation is commonly used to describe water flow in partially saturated soils. The three-dimensional form of this equation is given by:

$$\frac{\partial(\rho_w\theta_w)}{\partial t} = \nabla\cdot(\rho_w\bar{\bar{K}}_w\nabla\phi) \qquad (1)$$

Where ρ_w (kg cm^{-3}) is water density, θ_w (cm^3 cm^{-3}) is the volumetric water content, $\bar{\bar{K}}_w$ (cm h^{-1}) is the hydraulic conductivity tensor, and ϕ (cm) is the total water potential. Eq. (1) describes the movement of water in a coordinate frame, termed spatial or Eulerian, that is fixed with respect to the experimenter. Even though Eq. (1) is, in principle, applicable to any soil, including deforming ones, its use in this latter context is particularly complex. This is due, in part, to the need to account continuously for the effect of the deformation on the spatial and temporal dependency of $\bar{\bar{K}}_w$ and ϕ, as well as of the boundary conditions under Eq. (1) is solved (e.g. Sposito and Giráldez 1976; Vauclin 1988).

For these reasons, it is preferable to describe the transport of water in swelling soils in a coordinate frame (termed referential, material, or Lagrangian), that is associated with the solid phase. Under these conditions, the fundamental water flow equation is given by (e.g., Raats and Klute 1968 a and b, 1969; Sposito and Giráldez 1976; Angulo Jaramillo 1989):

$$\rho_d\frac{\partial\left[\dfrac{\rho_w\theta_w}{\rho_d}\right]}{\partial t} = \nabla_s\cdot\left(\rho_w\bar{\bar{K}}_{w/s}\nabla_s(\phi)F_s^{-1}\right)F_s^{-1} \qquad (2)$$

where ρ_d (kg cm^{-3}) is the dry bulk density, $\bar{\bar{K}}_{w/s}$(cm h^{-1}) is the hydraulic conductivity tensor relative to the solid phase, and the subscript s in the operator ∇_s indicates that the spatial derivatives are with respect to Lagrangian coordinates. Eq. (2) differs from Eq. (1) by the presence of F_s, the transformation gradient tensor. Its components are given by (Truesdell and Toupin 1960; Baveye 1992):

$$F_{s_{ij}} = \frac{\partial x_i}{\partial X_j} \qquad (3)$$

where x_i and X_j are a spatial coordinate and a material coordinate, respectively. The Jacobian determinant of the transformation gradient tensor is given by (Euler 1762):

$$J_s \equiv \det|F_s| = \frac{\rho_r}{\rho_d} \qquad (4)$$

where ρ_r(kg cm^{-3}) is the soil density in a reference state r. The last equality is not a constitutive assumption, but results directly from the microscopic mass balance equation (e.g., Baveye 1992).

A further difference between Eqs. (1) and (2) is the inclusion in the latter of an additional component Ω (cm) in the expression of the total water potential ϕ, representing the overburden potential. With this added term, the total water potential is given by (e.g., Philip 1969; Sposito and Giráldez 1976):

$$\phi = h - z + \Omega \qquad (5)$$

where h (cm) is the matric potential and z is the gravitational potential (positive downward). The

overburden Ω is expressed in material coordinates by:

$$\Omega = \bar{V}\left[P_0 + \int_0^z \gamma(F_s)_z dZ\right] \quad (6)$$

where $\bar{V}$ is the slope of the deformation curve, P_0 (cm) accounts for any external load, γ is the apparent wet specific density of overlying soil ($\gamma = \theta_w + \frac{\rho_d}{\rho_w}$), and Z is the vertical material coordinate.

In spite of the presence of F_s and Ω in Eq. (2), this equation is still formally similar to Eq. (1). Consequently, the numerous computational methods and general deductions that have been developed for the Richards equation may be applied when using Eq, (2) to describe the transport of water through deforming soils.

For convenience in applications, Eq. (2) is often recast in a form that involves as independent variables the moisture ratio ϑ (volume of water/volume of solid) and the ratio e (volume of void / volume of solid). These variables present the advantage that they are expressed relative to the volume of solid, which remains constant in swelling soils. They are related to the specific density of soil solids (ρ_s), the dry bulk density (ρ_d), and volumetric water content (θ_w) via the following relations:

$$\vartheta = \theta_w \frac{\rho_s}{\rho_d} \quad (7a)$$

$$e = \frac{\rho_s}{\rho_d} - 1 \quad (7b)$$

Introducing these variables in Eq. (2) and assuming the water to be incompressible (with $\rho_w = 1$ g/cm^{-3}), one obtains the following form of the water flow equation in a Lagrangian coordinate frame:

$$\frac{1}{1+e}\frac{\partial \vartheta}{\partial t} = \nabla_s \cdot (\bar{\bar{K}}_{w/s} \nabla_s(\phi) F_s^{-1}) F_s^{-1} \quad (8)$$

Except for a cosmetic change in the notations, Eq. (8) is equivalent to Eq. (2).

One-Dimensional Case

Expressions for the transformation gradient tensor F_s presented in the soil physics literature correspond to one-dimensional movement of the soil solid particles (Raats and Klute 1969; Smiles and Rosenthal 1968; Baveye 1992). They are given by the general form:

$$F_s = \begin{bmatrix} 1 & 0 & 0 \\ 0 & 1 & 0 \\ 0 & 0 & \rho_r/\rho_d \end{bmatrix} \quad (9)$$

where ρ_r, as in Eq. (4), is the soil density in a reference state r. Smiles and Rosenthal (1968) consider a hypothetical state with zero porosity of a soil, in which case $\rho_r = \rho_s$. Raats and Klute (1969), on the other hand, refer to an initial state of soil porosity, $\rho_r = \rho_{d_0}$ is the initial dry bulk density.

In practical applications, this second approach presents the advantage that it does not require the evaluation of ρ_s, since the reference state corresponds to an actual configuration of the system, for which measured data are available (e.g., Sposito et al. 1976; Baveye et al. 1989). Nevertheless, when the water flow equation is written in terms of ϑ and e, Smiles and Rosenthal's (1968) reference state has the appealing feature that it leads to a very concise formulation for the water flow equation because of simplifications resulting from Eq. (7b). Indeed, taking $\rho_r = \rho_s$ and substituting Eq. (9) in the one-dimensional version of Eq. (8), one obtains the following equation (Philip 1969):

$$\frac{\partial \vartheta}{\partial t} = \frac{\partial}{\partial Z}\left[\frac{K_{w/s}}{1+e}\frac{\partial \phi}{\partial Z}\right] \quad (10)$$

where $K_{w/s}$ is the principal value of the conductivity tensor.

Three-Dimensional Case

The deformation gradient tensor F_s in Eq. (9) is restricted to one-dimensional situations. The new form of the tensor F_s, introduced in the pres-

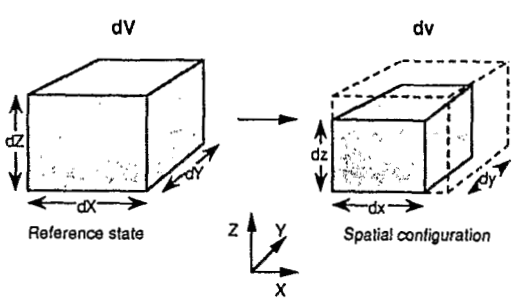

Fig. 1. Schematic illustration of the three-dimensional deformation of a soil volume, when the reference state is taken as the initial configuration of the soil, at the onset of shrinkage.

ent paper to deal with anisotropic deformation, is predicated by the assumption that soil deformation is isotropic in directions perpendicular to the z axis ("hypothesis 1"). In a sense, one might argue that this situation corresponds to axially symmetric two-dimensional deformation, but we shall continue to refer to the deformation as three-dimensional deformation.

Let us consider an elementary soil volume dV(dV = dXdYdZ) that undergoes a deformation such that its volume becomes dv (dv = dxdydz) (Fig. 1). If the deformation occurs without mass variation, one has:

$$dV = \frac{1 + e_r}{1 + e}\, dV \tag{11}$$

where e_r and e are the void ratios of the elementary soil volumes dV and dv, respectively.

The volume change described by Eq. (11) may be related to changes in either one of the three principal dimensions of the soil volume dv along x, y, z by using Bronswjik's (1990) dimensionless geometry factor, r_s, defined in the z direction by:

$$\left[1 - \frac{(dV - dv)}{dV}\right] = \left[1 - \frac{(dZ - dz)}{dZ}\right]^{r_s} \tag{12}$$

When the deformation occurs only in the vertical (z) direction, $r_s = 1$. In the case of isotropic deformation, $r_s = 3$. If vertical deformation is predominant then $1 < r_s < 3$; otherwise $r_s > 3$.

Eq. (11), Eq. (12), and hypothesis 1 lead to the following constitutive relations for the changes in the spatial coordinates x, y, z.

$$\begin{cases} dx = dX\left[\dfrac{1 + e}{1 + e_r}\right]^{\frac{1}{2}(1-1/r_s)} \\ dy = dY\left[\dfrac{1 + e}{1 + e_r}\right]^{\frac{1}{2}(1-1/r_s)} \\ dz = dZ\left[\dfrac{1 + e}{1 + e_r}\right]^{1/r_s} \end{cases} \tag{13}$$

where X, Y, Z represent the material coordinates. These relations are derived here for the first time. It provides a new coordinate transformation that allows one to take three-dimensional deformation.

The relations of Eq. (13) imply that each coordinate x, y, and z, depends only on X, Y, and Z, respectively. Therefore, the non-diagonal terms of F_s are identically equal to zero, and the transformation gradient tensor F_s becomes:

$$F_s = \begin{bmatrix} \left[\dfrac{1 + e}{1 + e_r}\right]^{\frac{1}{2}(1-1/r_s)} & 0 & 0 \\ 0 & \left[\dfrac{1 + e}{1 + e_r}\right]^{\frac{1}{2}(1-1/r_s)} & 0 \\ 0 & 0 & \left[\dfrac{1 + e}{1 + e_r}\right]^{1/r_s} \end{bmatrix} \tag{14}$$

The state of reference, r, in this expression may be chosen arbitrarily, depending on available data. For example, it can be the initial state (*cf.* Fig. 1) or the configuration at the shrinkage limit.

Three-Dimensional Deformation and One-Dimensional Water Flow

In many situations of practical interest (e.g., evaporation, infiltration in field soils as long as no cracks are present), water flow in deforming soils is predominantly one-dimensional in the direction of the gravitational force. This will also be the case in the experiments described in the next section. Therefore, we introduce a further hypothesis in the theory developed earlier, namely that points within a given horizontal plane, at an elevation z, have identical soil water potentials (hypothesis 2).

With this hypothesis, the introduction of F_s (Eq. (14)) in Eq. (8) provides a new form of the general equation of water flow. Using Eq. (5) for Φ and Eq. (6) for Ω and assuming no external load ($P_0 = 0$), the water flow equation becomes:

$$\frac{\partial \vartheta}{\partial t} = I(1 + e)\frac{\partial}{\partial Z}\left[T_1 \frac{\partial \vartheta}{\partial Z} - T_2\right] \tag{15}$$

where:

$$I = \left[\frac{1 + e_r}{1 + e}\right]^{1/r_s} \tag{16a}$$

$$T_1 = K_{w/s} I\left[\frac{\partial h}{\partial \vartheta} + \left(\int_0^Z \gamma I^{-1} dZ\right)\frac{\partial \bar{V}}{\partial \vartheta}\right] \tag{16b}$$

$$T_2 = K_{w/s}(1 - \gamma \bar{V}) \tag{16c}$$

When the reference state is taken as the configuration of the soil before shrinkage occurs, Eq. (15) corresponds to the water flow equation derived by Kim et al. (1992). The numerical solution of Eq. (15) may be carried out by using a classical finite-difference discretization scheme. We adopted an implicit discretization scheme with an

explicit linearization of coefficients. Because of the depth-dependent lateral deformation of the soil, however, the discretization has to account explicitly for the cross-sectional area of each spatial element so as to preserve mass balance (see Appendix for the discretization).

MATERIALS AND METHODS

Model Calibration with 1-D Data

Experimental Setup

The data of Angulo Jaramillo (1989) were obtained for a series of laboratory vertical infiltration experiments on a compacted mixture of loam and bentonite (20% by mass). The sample was placed in a cylinder 6 cm in diameter and 6 cm in height. A mobile piston connected to a porous plate was placed on top of the sample. This setup allowed the sample to swell freely. A hydraulic head was applied at the upper surface of the sample, and a microtensiometer cup measured the pressure head at 1.5 cm from the bottom of the sample. The spatial and temporal evolution of volumetric moisture content and bulk density within the soil sample were measured at 0.5-cm intervals with two radioactive sources (^{241} Am and ^{137}Cs) emitting colinear gamma rays. A comparator was used to measure changes in sample light.

Given the design of Angulo Jaramillo's (1989) experiments, soil deformation was allowed to take place only in the vertical direction, and consequently the geometry factor r_s was set equal to unity.

Experimental Hydraulic Characteristics of the Soil

The measured profiles of volumetric water content and bulk density, and the pressure heads at different times, allowed the calculation of the soil hydraulic characteristics, i.e., the moisture retention curve, the hydraulic conductivity, and the swelling curve (Angulo Jaramillo 1989; Kim et al. 1995).

The gamma ray system provided a relation between volumetric moisture content (θ_w) and dry bulk density (ρ_d). Because we used the variables moisture ratio (ϑ) and void ratio (e), as in Eq. (15), we operated the transformations of Eq. (7a) and (7b). We considered the swelling curve of the surface layer because it reached the highest values of water content.

In swelling soil, tensiometric measurement is the sum of matric potential (h) and overburden potential (Ω) (Talsma 1974). The overburden potential was calculated with Eq. (6) from the apparent wet specific density (γ) of the overlying soil and the swelling curve slope ($\bar{V}$). Angulo Jaramillo (1989) deduced the matric potential (h) from tensiometric lecture and calculated overburden potential at 1.5 cm from the bottom of the sample. The volumetric water content (θ_w) and the bulk density (ρ_d) measured at the same level as the tensiometric measurement provided the relation between moisture ratio (ϑ) (with Eq. (7a)) and matric potential (h).

Argullo Jaramillo (1989) showed that Eulerian and Langrangian approaches provided very similar hydraulic conductivity curves. In the Lagrangian approach, the hydraulic conductivity was calculated from the material diffusivity ($D_m = D_{w/s}/(1 + e)$) by Philip (1969) and Angulo Jaramillo (1989):

$$K_{w/s} = D_m(\partial\theta_w/\partial h)\theta_s^{-2}[1 - (\theta_w/\theta_s)(d\theta_s/d\theta_w)] \quad (17)$$

This relation gives $K_{w/s}$ from the swelling curve expressed in terms of θ_s and θ_w, the retention curve, and the material diffusity, D_m, which can be calculated with the Boltzman variable (ξ_m) by (Yong and Warkentin 1975):

$$D_m = -\frac{1}{2}\frac{d\xi_m}{d\vartheta}\int_{\vartheta_0}^{\vartheta}\xi_m(\vartheta)d\vartheta \quad (18)$$

Boundary Conditions

The following boundary conditions were used for the calibration of the numerical model with Angulo Jaramillo's (1989) data. The gaseous phase was assumed to be at atmospheric pressure throughout the column. The top boundary condition, of the Cauchy type, was given by the following expression:

$$q_{surf}(t) = \frac{K_p}{d}\left[h_0 - \delta z(t) - h_{sp}(t)\right] \quad (19)$$

where q_{surf} (cm h^{-1}) is the water flux through the soil surface, K_p (cm h^{-1}) is the saturated hydraulic conductivity of the porous plate, d (cm) is the thickness of the porous plate ($K_p/d = 1.4\ 10^{-4}$ h^{-1}), h_0 (cm) is the constant hydraulic head relative to the initial soil surface ($h_0 = 11.846$ cm), δz (cm) is the displacement of the soil surface and h_{sp} (cm) is the hydraulic head between the soil and the porous plate. At the lower end of the soil sample, a Neuman condition with zero flux was imposed.

Models for Hydraulic Characteristics

The water flow model, whose general equation is given by Eq. (15), requires knowledge of

the soil hydraulic characteristics. To this end, the experimental data obtained during the infiltration experiment were fitted with various mathematical expressions.

For the swelling curve, we selected the model of Braudeau (1988 a and b) because this model appears to be the most versatile of all available models. Braudeau's model takes into account the three types of deformation generally identified in swelling soils. In the direction of increasing water ratio, these are, successively, the residual, principal, and structural deformation regimes (Fig. 2) Braudeau's (1988) model is based on the assumption that the soil consists of clayey microaggregates separated from each other and from the other soil constituents by a network of macropores. Braudeau (1988) and Braudeau and Touma (1995) identify four points on the swelling curve: shrinkage limit (SL), "air entry" in the microaggregates (AE), the limit of contribution of macroporosity to shrinkage (LM), and the maximum swelling of the microaggregates (MS). These authors propose a mathematical expression (Table 1) that involves the coordinates of these four points along with the slope (K_r) of the linear part of the principal deformation and the slope (K_0) of the linear part of the structural deformation. We fitted this experimental swelling curve with Braudeau's (1988) model (Fig. 3a). The fitted values of parameters are given in Table 2.

For the water characteristic curve, we selected Van Genuchten's (1980) equation with Burdine's (1953) condition, and for the hydraulic conductivity, we chose Brooks and Corey's (1964) parametric equation, because of the documented applicability of these expressions to a wide range of soils (Fuentes et al. 1992). In terms of the moisture ratio ϑ, Van Genuchten's (1980) equation is given by:

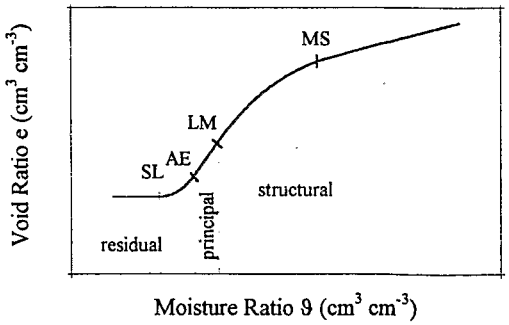

Fig. 2. Experimental shrinkage curve and its transition points (adapted from Braudeau (1988a)).

$$Se(h) = \frac{\vartheta - \vartheta_r}{\vartheta_s - \vartheta_r} = \left[1 + (\alpha h)^n\right]^{-m} \quad (20)$$

where Se is the effective saturation, ϑ_r (cm^3cm^{-3}) and ϑ_s (cm^3cm^{-3}) are the residual and saturated moisture ratios, respectively, and α (cm^{-1}), n, and m are empirical parameters. The Burdine's (1953) condition states that ($m = 1 - 2/n$). Brooks and Corey's (1964) equation for the hydraulic conductivity is expressed as:

$$K(\vartheta) = K_s(Se)^B \quad (21)$$

where K_s (cm h^{-1}) is the saturated hydraulic conductivity and B is an empirical parameter. We fitted the experimental retention curve (Fig. 3b) and hydraulic conductivity curve (Fig. 3c) with Van Genuchten's (1980) model and Brooks and Corey's (1964) model, respectively. The fitted values of parameters are provided in Table 2.

Sensitivity Analysis of 3-D Model

We used the previously parametrized hydraulic characteristics to evaluate the sensitivity of our water flow model to the geometry factor r_s. We simulated infiltration and drainage experiments with the same deformation curve but with different assumptions regarding the anisotropy of the soil. These assumptions resulted in the simulation of vertical deformation only ($r_s = 1$), vertical deformation that was twice of that occurring in each horizontal direction ($r_s = 2$), isotropic deformation ($r_s = 3$), vertical deformation that was half of that in each horizontal direction ($r_s = 5$), and a situation involving horizontal deformation ($r_s = 100$) almost exclusively.

For the simulated infiltration experiment, the initial and boundary conditions and the initial dimension of the sample were the same as those in Angulo Jaramillo's experiment. However, $r_s > 1$, so that the sample was allowed to deform laterally. For the simulated drainage experiment, a Neuman condition with zero flux was imposed at the top, and a Dirichlet condition with −350 cm of water pressure head at the bottom. The sample had the same initial dimension as found previously and a uniform initial water content profile near saturation.

RESULTS AND DISCUSSIONS

Model Calibration with 1-D Data

Experimental and simulated results were compared in order to determine whether the numerical model could be calibrated reasonably easily using Angulo Jaramillo's (1989) data. A com-

TABLE 1

Parametric equations associated with the different deformation regimes in Braudeau's (1988) model.

Deformation regimes	Equations of the Braudeau model
Region SL	$e = e_{SL}$
Region SL-AE	$e = e_{SL} + K_r\left[\frac{\vartheta_{AE} - \vartheta_{SL}}{\exp(1) - 1}(\exp V_n - 1 - V_n)\right]$ with $V_n = \frac{\vartheta - \vartheta_{SL}}{\vartheta_{AE} - \vartheta_{SL}}$
Region AE-LM	$e = Kr(\vartheta - \vartheta_{AE}) + e_{AE}$
Region LM-MS	$e = \frac{\vartheta_{LM} - \vartheta_{MS}}{\exp(1) - 1}\left[(K_r - K_0)(\exp(V_m) - \exp(1)) - \frac{\vartheta - \vartheta_{LM}}{\vartheta_{LM} - \vartheta_{MS}}(K_r - K_0 \exp(1))\right] + e_{LM}$ with $V_m = \frac{\vartheta - \vartheta_{MS}}{\vartheta_{LM} - \vartheta_{MS}}$
Beyond MS	$e = K_0(\vartheta - \vartheta_{MS}) + e_{MS}$

parison between experimental and simulated profiles of volumetric water content and dry bulk density is presented after 133.3 and 533.3 of infiltration (Fig. 4). Experimental data are reported with their maximum theoretical error (0.06 cm^3cm^{-3}) (*cf* analysis in Angulo Jaramillo 1989).

The first simulated profile, after 133.3 falls within the experimental error intervals for both the volumetric water content and the dry bulk density. At this stage the surface rise is also simulated reasonably well. The second simulated profiles, after 533.3, underestimated the volumetric water content in the lower half of the soil sample and overestimated the dry bulk density. However, the experimental and simulated curves have similar sigmoidal shapes. The simulated surface rise (1.75 cm) was a bit higher than the experimentally observed one (1.35 cm). There are several reasons for this discrepancy between measured and computed results. One is that the large experimental error associated with the experimental data may include errors in the determination of the hydraulic properties. This error accumulation may have repercussions on the simulated results. Moreover, the approximations caused by the use of models (Van Genuchten 1980; Brooks and Corey 1964; Braudeau 1988) explain some of the differences between simulated and measured results. Another reason for the differences is that the actual hydraulic characteristics may be heterogeneous as a result of the overburden pressure that may not be identical in each layer within the soil sample.

Scatterplots were constructed from the computed and observed profile data for the volumetric water content and the dry bulk density (Fig. 5). These diagrams reflect the general tendency of the numerical model to overestimate the volumetric water content and to underestimate the dry bulk density, as already evidenced in Fig. 4. Nevertheless, the coefficients of determination were equal to 0.9 for the volumetric water content and 0.77 for the dry bulk density. Thus, in spite of slight de-

TABLE 2

Values of selected model parameters estimated on the basis of the experimental data of Angulo Jaramillo (1989).

Mathematical expressions	parameter values
Swelling curve (model of Braudeau 1988)	
ϑ_{SL}; $e_{SL}(cm^3/cm^3)$	0.45; 0.71
ϑ_{AE}; $e_{AE}(cm^3/cm^3)$	0.98; 0.91
ϑ_{LM}; $e_{LM}(cm^3/cm^3)$	4.58; 4.06
K_r	0.88
Moisture retention characteristic (model of Van Genuchten 1980)	
$\vartheta_s(cm^3/cm^3)$	4.07
$\vartheta_r(cm^3/cm^3)$	0.706
$\alpha(cm^{-1})$	−0.0563
n	3.036
Hydraulic conductivity (model of Brook and Corey 1964)	
$\vartheta_s(cm^3/cm^3)$	4.07
$\vartheta_r(cm^3/cm^3)$	0
$K_s(cm/h)$	0.00035
B	2.772

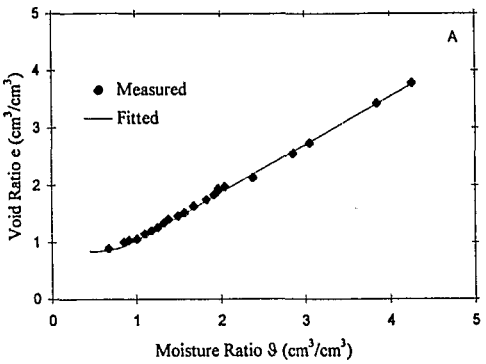

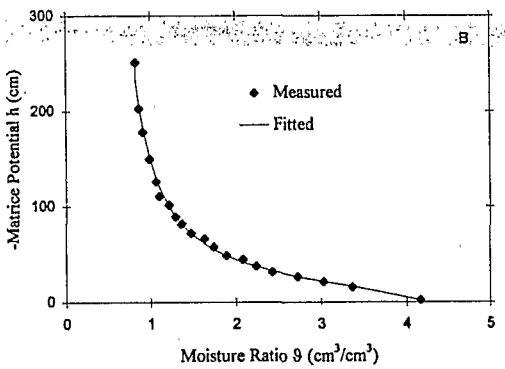

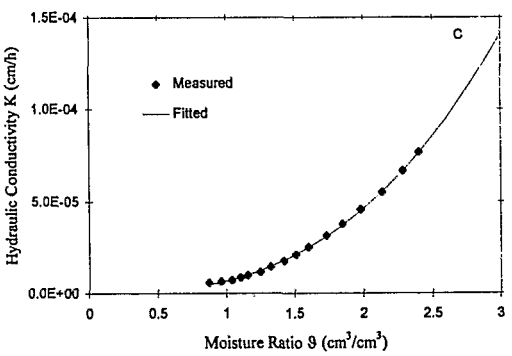

Fig. 3. Comparison of measured and fitted curves for the shrinkage curve (A), the retention curve (B) and the hydraulic conductivity curve (C).

viations, the numerical results appear to be in reasonably good agreement with the measured data.

Sensitivity Analysis of 3-D Model

We tested the sensitivity of the solutions of the water flow equation (Eq. 15) to variation in r_s factor by simulating infiltration (Eq. (6a) and (6b)) and drainage (Eq. (6c) and (6d)) experiments.

Figure 6a shows that, at the end of the infiltration (533.3 for each profile), an increase in r_s leads not only to a decrease in the final sample height but also to a shift in the volumetric water content profile in the direction of higher water contents. Figure 6b shows that the infiltrated water volume increases with r_s, in all likelihood because of a larger top cross-sectional area through which water infiltrates.

The volumetric water content profiles at the end of the drainage (533.3 h for each profile) for different values of r_s are presented in Fig. 6c. The increase in r_s causes a smaller decrease in sample height at the final time of observation, and a shift in profiles in the direction of higher water con-

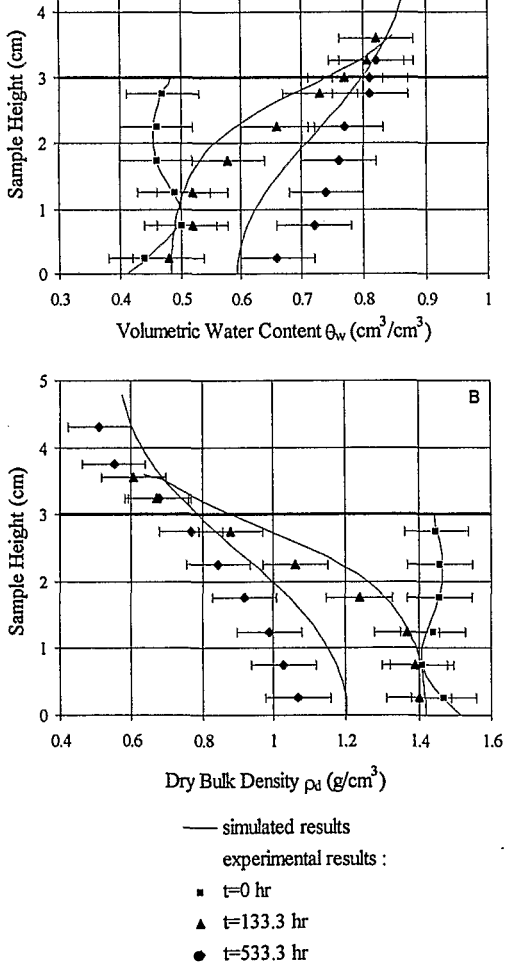

Fig. 4. Comparison of experimental and simulated profiles of the volumetric water content (A) and the dry bulk density (B) for the infiltration experiment of Angulo Jaramillo (1989).

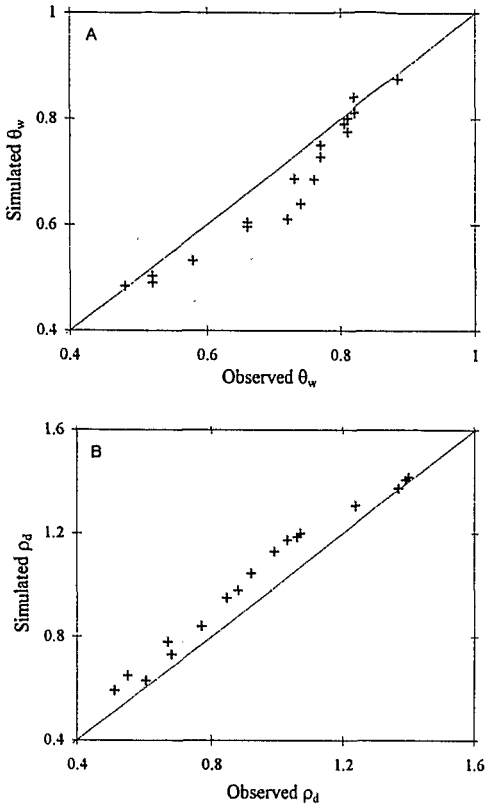

Fig. 5. Scatterplots of experimental and simulated data of the volumetric water content (A) and dry bulk density (B) for the infiltration experiment of Angulo Jaramillo (1989)

tents, as in the infiltration case. This shift in profiles to higher water stems from a decrease of the cumulative outflow water volume (Fig. 6d) as a result of the smaller lower surface of the soil sample.

Interestingly, in all cases in Fig. 6, the largest difference between curves associated with different r_s values occur when r_s goes from 1 to 2, i.e. for relatively small departures from strictly vertical deformation.

The results presented above show that simulations carried out with different values of r_s can lead to significant differences in terms of water distribution, height, and total water content of the sample. The results obtained from 1-D simulation ($r_s = 1$) and from 3-D simulation ($r_s > 1$) are qualitatively different. We conclude that taking into account the anisotropy of the deformation in the water flow model is a necessity in this type of swelling soils when the deformation is not strictly vertical. Moreover, an inaccurate estimation of r_s (in the range $2 < r_s < 5$) may lead to a poor simulation of water flow and deformation. Therefore, it is important not only to measure the geometry factor with accuracy but to do so under conditions as close as possible to those of the simulated experiment.

Water flow models may be used not only as predictive tools but also to evaluate the hydraulic conductivity of soils. Most of the methods used in this case require one to solve the water flow equation numerically. In inverse methods, comparison between measured and simulated values of several selected variables allows the determination of the optimal parameter values. From the results obtained above, it appears that introducing an erroneous value of the geometry factor r_s into the model may lead to very different simulations of water distribution, surface height, and total water volume of the sample and, therefore, to unreliable estimates of the hydraulic properties. A similar conclusion pertains to the more direct methods, in which numerical resolution of the water flow equation, subject to specified boundary conditions, leads to an evaluation of the hydraulic parameters.

CONCLUSION

The key contributions of the present article are to be found in Eq. (13) and in the results of the sensitivity analysis illustrated by Fig. 6. Equation (13) provides a new coordinate transformation that allows one to take three-dimensional deformation into account in the description of water flow through swelling/shrinking soils. The soil deformation is assumed to be horizontally isotropic, but anisotropic otherwise. The coordinate transformation involves a geometric factor r_s, which takes values in the range $1 < r_s < \infty$.

To estimate the impact of the geometric factor on the flow of water in deforming soils, a numerical finite-difference code based on a generalized water flow equation was first calibrated with a set of one-dimensional infiltration data obtained by Angulo Jaramillo (1989). The calibrated parameter values were then used in a sensitivity analysis of the three-dimensional model. As expected, this analysis shows that the height of the soil surface is controlled by the value of the geometry factor r_s (cf. Fig. 6). At the same time, r_s also has a significant effect on the distribution of water and on the total volume of water in the soil samples. Hence, it is important to take the geometric factor r_s explicitly into account when

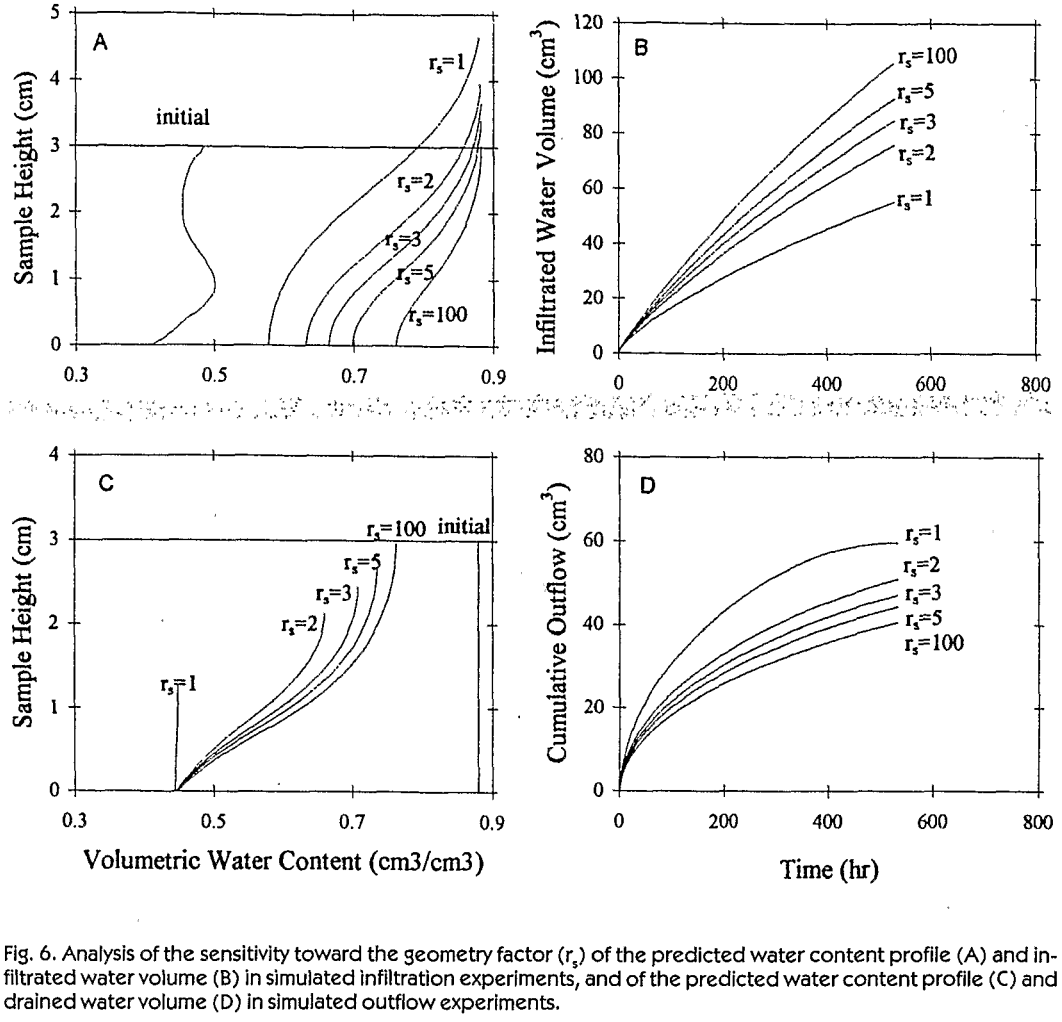

Fig. 6. Analysis of the sensitivity toward the geometry factor (r_s) of the predicted water content profile (A) and infiltrated water volume (B) in simulated infiltration experiments, and of the predicted water content profile (C) and drained water volume (D) in simulated outflow experiments.

predicting water flow in anisotropically deforming soils or estimating the hydraulic properties of soils.

REFERENCES

Angulo Jaramillo, R. 1989. Caractérisation hydrodynamique de sols déformables partiellement saturés: Etude expérimentale à l'aide de la spectrométrie gamma double source. Unpublished Ph.D. dissertation. Institut National Polytechnique de Grenoble. France.

Baveye, P. 1992. Operational aspects of the mechanics of deforming porous media: Theory and application to expansive soils. *In* T. Karalis (ed.). Mechanics of swelling. Springer-Verlag, Berlin, pp. 79–96.

Baveye, P., C. W. Boast, and J. V. Giráldez. 1989. Use of referential coordinates in deforming soils. Soil Sci. Soc. Am. J. 53:1338–1343.

Braudeau, E. 1988a. Equation généralisée des courbes de retrait d'échantillons de sols structurés. C. R. Acad. Sci. Sér. 2. 307:1731–1734.

Braudeau, E. 1988b. Essai de caractérisation quantitative de l'état structural d'un sol basé sur l'étude de la courbe de retrait. C. R. Acad. Sci. Sér. 2. 307:1933–1936.

Braudeau, E., and J. Touma. 1995. Modeling shrinkage of unconfined soil cores. *In* Vadose Zone Hydrology: Cutting Across Disciplines. University of California, Davis, USA, Sept., pp. 11–12.

Bronswijk, J. J. B. 1990. Shrinkage geometry of a heavy clay soil at various stresses. Soil Sci. Soc. Am. J. 54:1500–1502.

Brooks, R. H., and A. T. Corey. 1964. Hydraulic properties of porous media. Hydrology Paper 3, Colo. State Univ., Fort Collins.

Burdine, N. T. 1953. Relative permeability calculations from pore-sized distribution data. Trans. Am. Inst. Miner. Metall. Pet. Eng. 198:7–77.

Douglas, E., E. McKyes, F. Taylor, S. Negi, and G. S. V. Raghavan. 1980. Unsaturated hydraulic conductivity of a tilled clay soil. Can. Agric. Eng. 22:153–161.

Euler, L. 1762. Recherches sur la propagation des ébranlements dans un milieu élastique (lettre de M. Euler à M. de La grange). Opera 10:255–263.

Fuentes, C. R., Haverkamp, and J. Y. Parlange. 1992. Parameter constraints on closed-form soil water relationships. J. Hydrol. 134:117–142.

Giráldez, J. V., G. Sposito, and D. Delgado. 1983. A general soil change equation. Soil Sci. Soc. Am. J. 47:419–422.

Kim, D. J., H. Vereecken, J. Feyen, M. Vanclooster, and L. Stroosnijder. 1992. A numerical model of water movement and soil deformation in a ripening marine clay soil. Modeling Geo-Biosphere Processes. 1:185–203.

Kim, D. J., J. Feyen, R. Angulo Jaramillo, and M. Vauclin. 1995. Comparison of Eulerian and Lagrangian approaches in soil deformation and water flow. Int. Conf. of Unsaturated Soils, Paris. 2:751–757.

Philip, J. R. 1969. Hydrostatistics and hydrodynamics in swelling soils. Water Resour. Res. 5:1070–1077.

Philip, J. R., and D. E. Smiles. 1969. Kinetics of sorption and volume change in three-component systems. Aust. J. Soil Res. 7:1–19.

Raats, P. A. C., and A. Klute. 1968a. Transport in soils: The balance of mass. Soil Sci. Soc. Am. Proc. 32: 161–166.

Raats, P. A. C., and A. Klute. 1968b. Transport in soils: The balance of momentum. Soil Sci. Soc. Am. Proc. 32:452–456.

Raats, P. A. C., and A. Klute. 1969. One-dimensional, simulations motion of the aqueous phase and the solid phase of unsaturated and partially saturated porous media. Soil Sci. 107:329–333.

Richards, L. A. 1931. Capillary conduction of liquids through porous mediums. Physics 1:318–333.

Rijniersce, K. 1983. A simulation model for physical soil ripening in the Ijsselmeerpolders. Lelystad, the Netherland, p. 216.

Smiles, D. E. 1974. Infiltration into a swelling material. Soil Sci. 117:140–147.

Smiles, D. E., and M. J. Rosenthal. 1968. The movement of water in swelling materials. Aust. J. Soil Res. 6:237–248.

Sposito, G., and J. V. Giráldez. 1976. On the theory of infiltration in swelling soils. Proceedings of the ISSS symposium on water in heavy soils. The Czechoslovak Scientific Technical Society, Prague, 1976, pp. 107–118.

Sposito, G., J. V. Giráldez, and R. J. Reginato. 1976. The theoretical interpretation of field observations of soil swelling through a material coordinate transformation. Soil. Sci. Soc. Am. J. 40:208–211.

Talsma, T. 1974. Moisture profiles in swelling soils. Aust. J. Soil Res. 12:71–75.

Truesdell, C. A., and R. A. Toupin. 1960. The classical field theories. Hand. Physik, III/1:226–793.

Van Genuchten, M. Th. 1980. A closed-form equation for predicting the hydraulic conductivity of unsaturated soils. Soil Sci. Soc. Am. J. 44:892–898.

Vauclin, M. 1988. Hydrodynamique des sols partiellement saturés, déformables. Les phénomènes de transfert dans les milieux poreux déformables. Collection "les colloques de L'INRA":63–113.

Yong, R. N., and Warkentin B. P. 1975. Soil properties and behavior. Elsevier Sci. Pub. Co., Amsterdam.

APPENDIX

DISCRETIZATION OF THE 1-DIMENSIONAL WATER FLOW EQUATION DURING 3-DIMENSIONAL DEFORMATION OF SOIL

The discretized form of the Eq. 15 is:

$$\frac{\vartheta_i^{k+1} - \vartheta_i^k}{dt} = I_i^k(1 + e_i^k)\frac{1}{dZ}$$

$$\left[\left[(T_1)_{i+1/2}^k\left[\frac{\vartheta_{i+1}^{k+1} - \vartheta_i^{k+1}}{dZ}\right] - (T_2)_{i+1/2}^k\right] - \frac{S_{i-1/2}^k}{S_{i+1/2}^k}\left[(T_1)_{i-1/2}^k\left[\frac{\vartheta_i^{k+1} - \vartheta_{i-1}^{k+1}}{dZ}\right] - (T_2)_{i-1/2}^k\right]\right]$$

where i refers to the depth increment and k refers to the time increment.

The cross-sectional area of the spatial element i, S_i^k, is calculated by:

$$S_i^k = I_1^k(1 + e_1^k)\frac{(V_s)_i^k}{dZ}$$

where $(V_s)_i^k$ is the solid particul volume of the element i.

SOIL SCIENCE

An Interdisciplinary Approach to Soils Research

June 1997 **CONTENTS** **Vol. 162 No. 6**